Topological and Multipolar Magnets and Spintronics

Satoru Nakatsuji

Dept. of Physics, University of Tokyo
Institute for Solid State Physics (ISSP), University of Tokyo
Institute of Quantum Matters (IQM), Johns Hopkins University

Trans-scale Quantum Science Institute, UTokyo

School of Science・ISSP・IPMU・Cryogenic Research Center

- Bringing together the world-class research infrastructures of the University of Tokyo, promoting educational exchanges and collaborative research with leading universities and institutions abroad.
- Advancing the conceptual framework of fundamental quantum science, creating quantum-technology innovations, and training future quantum-science experts that may significantly benefit our society.

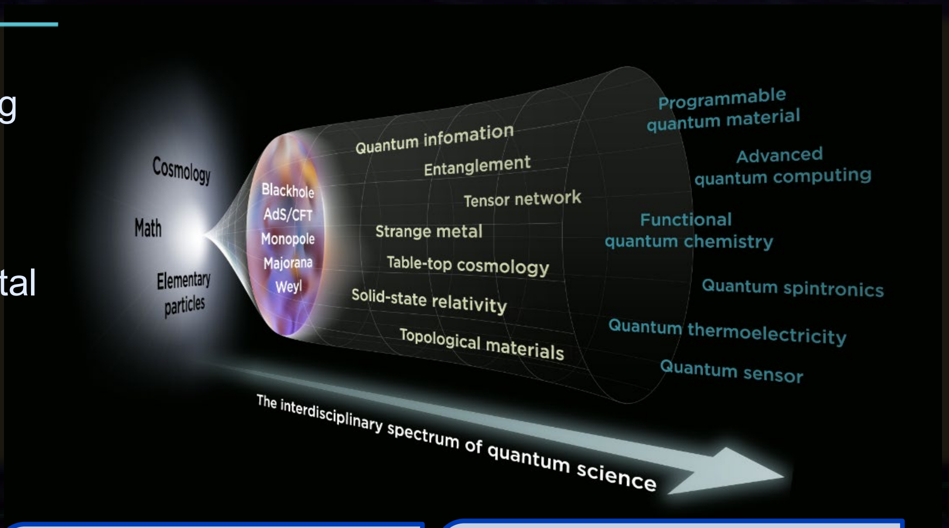

Research topics and expertise with excellent breadth and depth

Projects involving global & academia-industry collaborations

Multicultural research team with English being the second official language

Join our team: We always welcome applications from international students and postdocs with diverse backgrounds

Quantum Materials and Spintronics, Nakatsuji Lab.

Univ. of Tokyo
Dept. of Phys. & ISSP



Johns Hopkins Univ.
Dept. Phys. & Astro.

Staff: 6, Post-doc: 4, Student: 12 (International 7), Adm:5

Activities of Young Researchers

APS

International Conferences, workshop


TSQS2022

Thin film & device fabrication :
Sputter, MBE, Photo litho, EB-litho, ...

Measurement:
XRD, Prober, Dilution ref., PPMS, MPMS, …



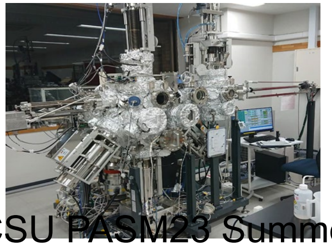

“Meanwhile, the Cosmos is rich beyond measure: the total number of stars in the Universe is greater than all the grains of sand on all the beaches of the planet Earth”

— Carl Sagan

Under a microscopic lens, quantum mechanical properties of electrons lead to a rich universe of exotic phases.

Topological Electronic Structure

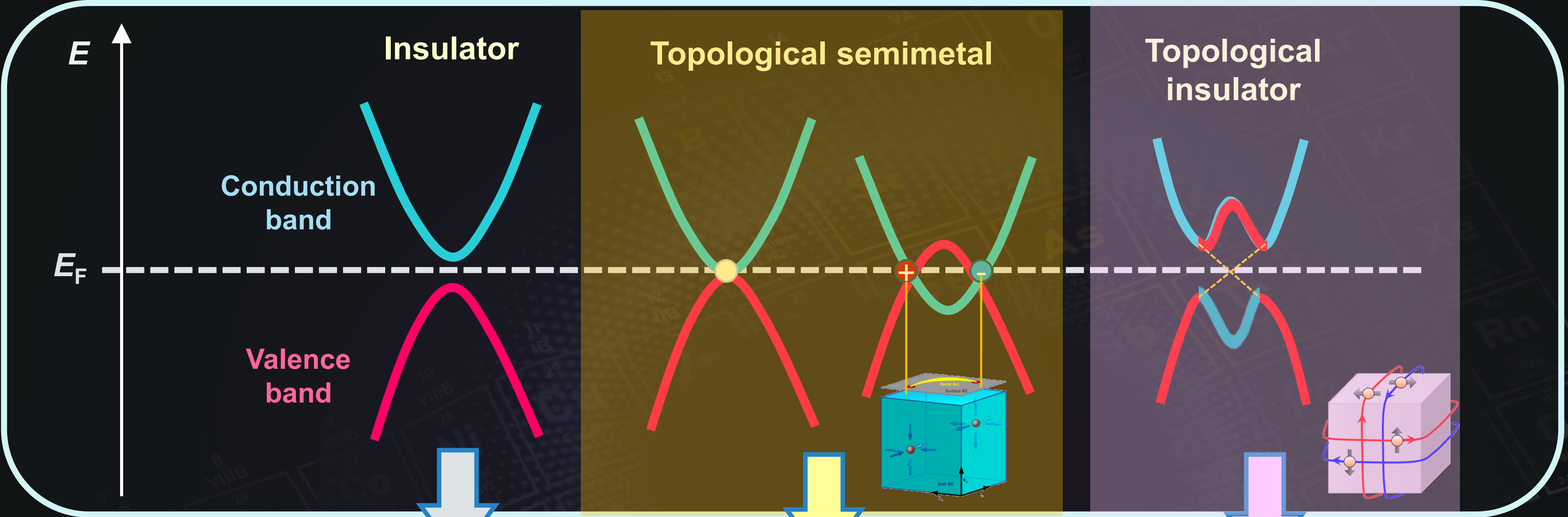

Diamond (Insulator)

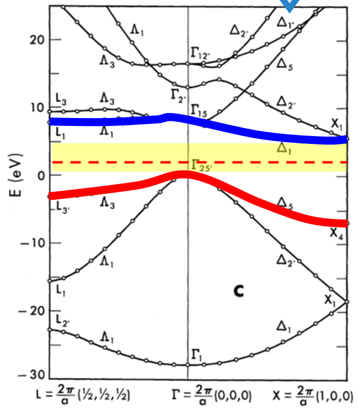

Cardona et al., Phys. Rev. **142**, 530 (1966).

Dirac **Nodal line** **Weyl**

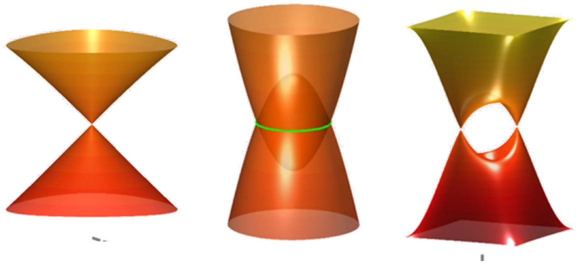

Armitage et al., RMP **90**, 015001 (2018);
Fu et al., APL Mater. **8**, 040913 (2020).
Nakatsuji & Arita, Annu. Rev. Cond. Matter Phys. **13**, 119 (2022).

Bi_2Se_3

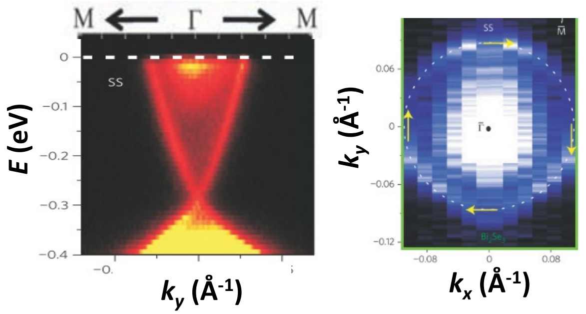

Hasan and Kane, RMP **82**, 3045 (2010).
Ando, JPSJ **82**, 102001 (2013).

Experimentally established in non/weakly-interacting electron systems

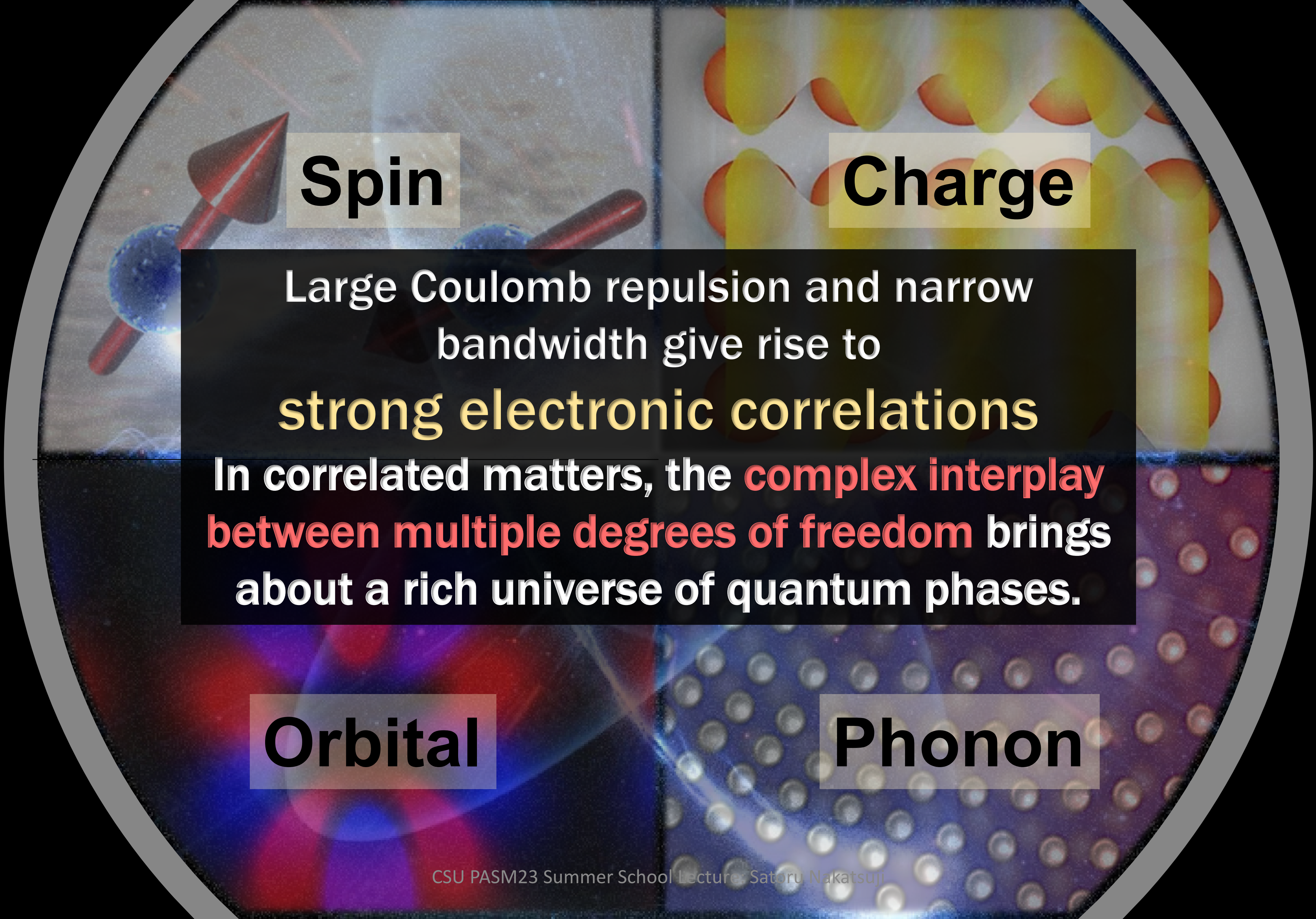

Large Coulomb repulsion and narrow bandwidth give rise to

strong electronic correlations

In correlated matters, the complex interplay between multiple degrees of freedom brings about a rich universe of quantum phases.

Traditional platforms: Spin-driven phenomena

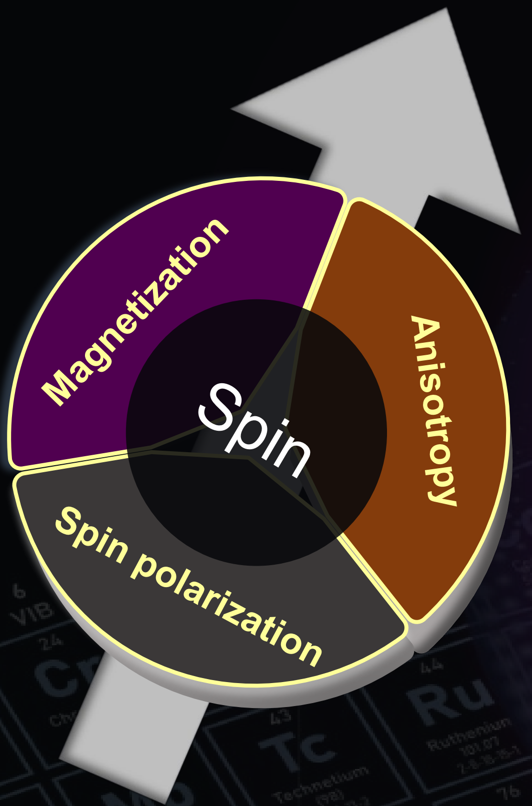

Quantum phenomena

- Superconductivity
- Strange metal and Quantum criticality
- Quantum liquids
- Kondo effect
- Metal-insulator transition

⋮

Functionalities & Applications

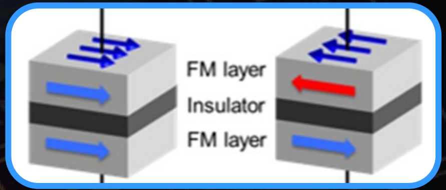

Ferromagnet-based nonvolatile memory

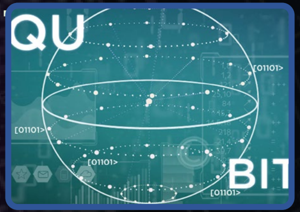

Quantum computing

Magneto-optics

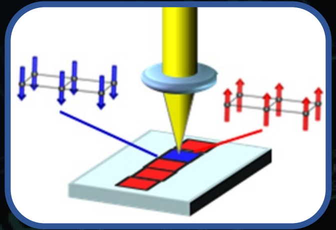

New platforms: blending topology with multipole physics

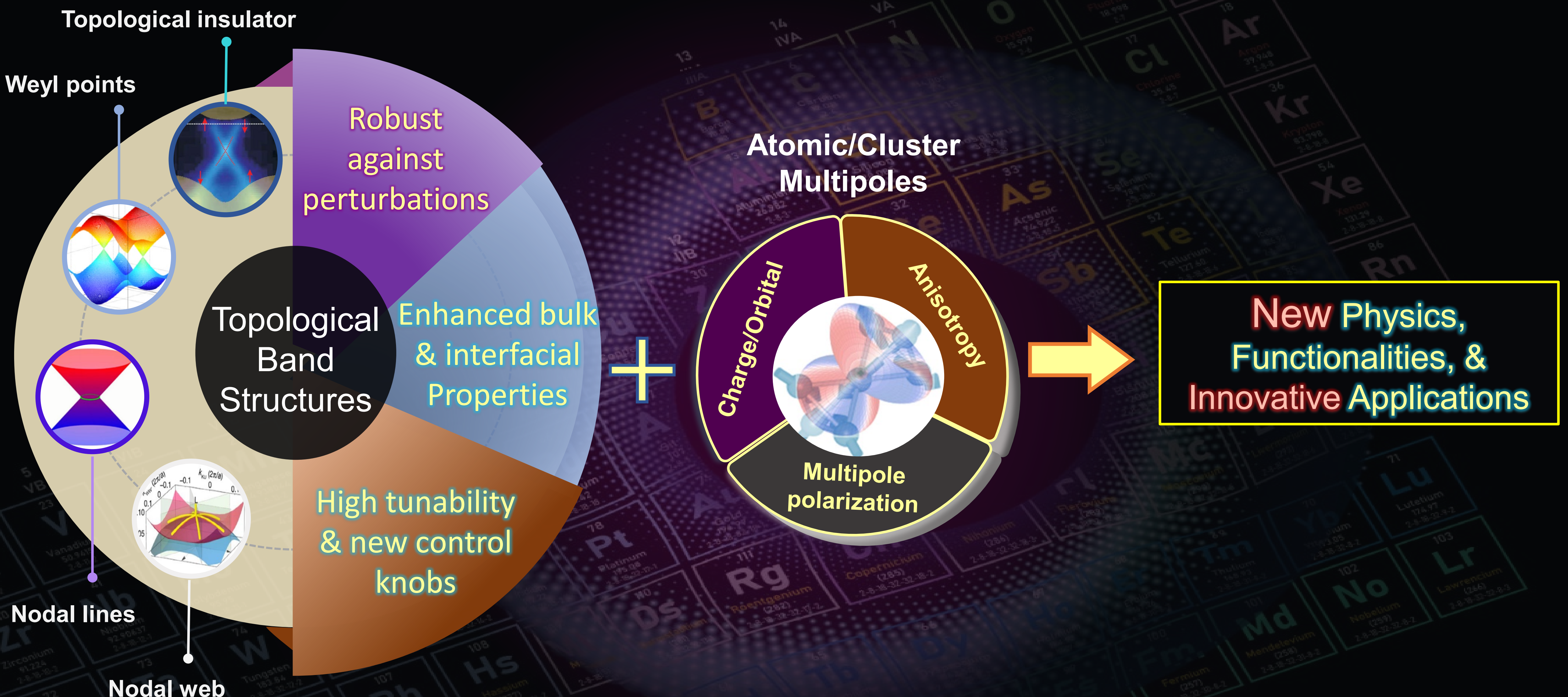

Plan

- Multipole Physics on Correlated Electron Systems
- Topological States in Magnetic Systems
- Physics of Antiferromagnetic Weyl Semimetals
- Physics of Multipolar Kondo Lattice Systems

Multipolar Expansion in electromagnetism

Maxwell equations:

$$\nabla \cdot \mathbf{E} = 4\pi\rho_e(\mathbf{r})$$ (Gauss' law for electricity)

Electric charge density

$\mathbf{E} = -\nabla\phi$ → $\nabla^2\phi = -4\pi\rho_e(\mathbf{r})$

Scalar potential field

$$\nabla \cdot \mathrm{B} = 0$$ (Gauss' law for magnetism)

→ $\nabla \cdot \mathrm{H} = 4\pi\rho_m(\mathbf{r})$

Magnetic charge density $\rho_m(\mathbf{r}) = -\nabla \cdot \mathbf{M}(\mathbf{r})$

$$\nabla \times \mathbf{E} = -\frac{1}{c}\frac{\partial \boldsymbol{B}}{\partial t}$$ (Faraday's law)

$$\nabla \times \mathrm{B} = \frac{1}{c}\left(4\pi\mathbf{j} + \frac{\partial \boldsymbol{E}}{\partial t}\right)$$ (Ampere's law)

$\mathbf{B} = \nabla \times \mathbf{A}$ → $\nabla^2\mathbf{A} = -\frac{4\pi}{c}\mathbf{j}(\mathbf{r})$

Vector potential field

Multipolar Expansion in electromagnetism

For regions outside an arbitrary source distribution, the scalar potential $\phi(\mathbf{r})$ and the vector potential $\mathbf{A}(\mathbf{r})$ admits a **multipolar expansion**:

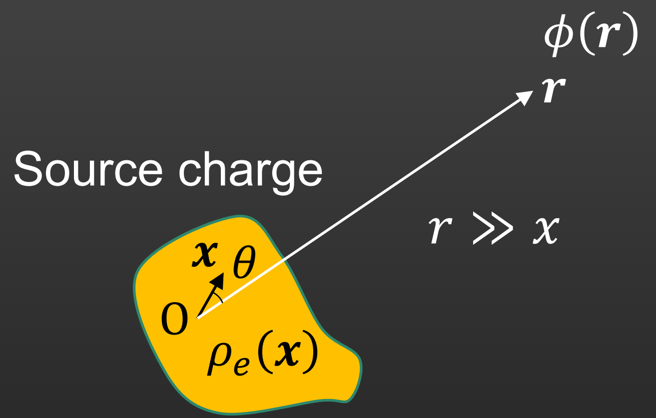

$$\phi(\mathbf{r}) = \sum_{l=0}^{\infty} \sum_{m=-l}^{l} \frac{1}{r^{l+1}} Z_{lm}(\hat{\mathbf{r}}) \boldsymbol{Q_{lm}}$$

→ Electric multipolar moments

Normalized spherical harmonics: $Z_{lm}(\hat{\boldsymbol{r}}) \equiv \sqrt{\frac{4\pi}{2l+1}} Y_{lm}(\hat{\boldsymbol{r}})$

$$\mathbf{A}(\mathbf{r}) = \sum_{l=0}^{\infty} \sum_{m=-l}^{l} \frac{1}{r^{l+1}} \frac{\mathbf{L} Z_{lm}(\hat{\mathbf{r}})}{il} \boldsymbol{M_{lm}}$$

→ Magnetic multipolar moments

$Q_{lm} \equiv \int d\boldsymbol{r}\, r^l Z_{lm}(\hat{\boldsymbol{r}})^* \rho_e(\boldsymbol{r})$ → Source charge density distribution

$M_{lm} \equiv \int d\boldsymbol{r}\, r^l Z_{lm}(\hat{\boldsymbol{r}})^* \rho_m(\boldsymbol{r})$ → Source magnetization density distribution

Multipolar Expansion in electromagnetism

Rank	Multipole	Expression for	Illustration
$l = 0$	Electric monopole	$\phi_{l=0}(\mathbf{r}) = \frac{q}{4\pi\varepsilon_0 r}$	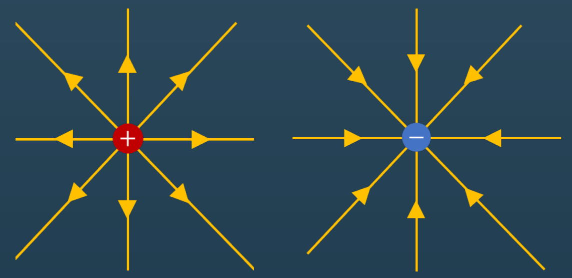
$l = 1$	Electric Dipole	$\phi_{l=1}(\mathbf{r}) = \frac{\boldsymbol{r}\cdot\boldsymbol{p}}{4\pi\varepsilon_0 r^3}$	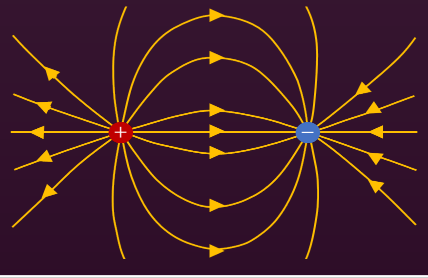
$l = 2$	Electric quadrupole	$\phi_{l=2}(\mathbf{r}) == \frac{3Q}{8\pi\varepsilon_0 r^3}$	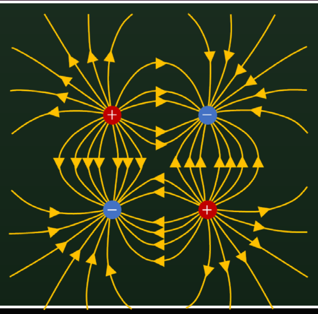

Atomic multipoles in a material

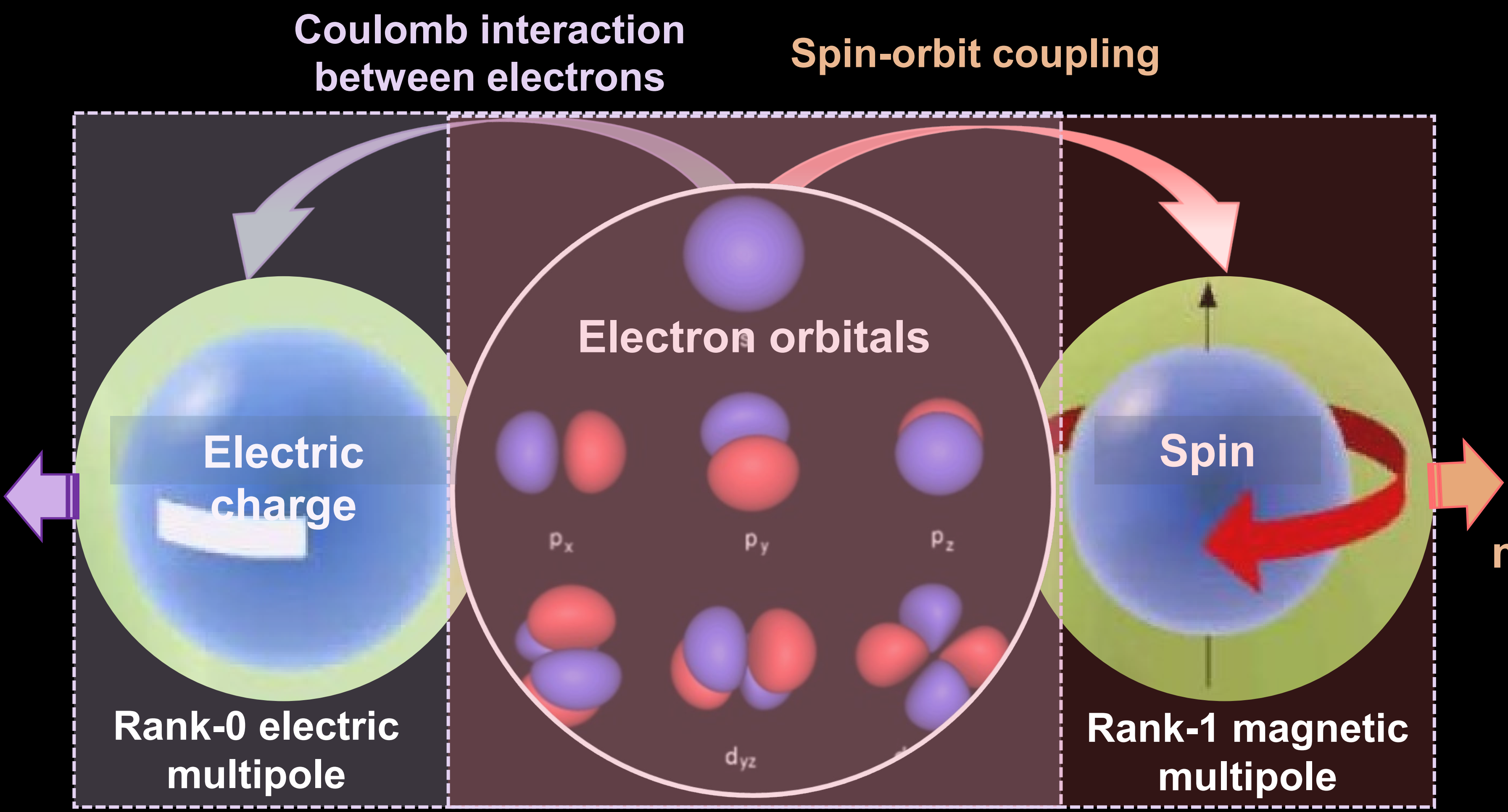

Electric multipoles
↓
Quantifies charge density distribution

Magnetic multipoles
↓
Quantifies magnetization density distribution

Multipoles characterize the localized charge and magnetization density distribution at an atomic site

Symmetry properties of atomic multipoles

Under inversion (spatial parity) transformation:
$$Q_{lm} \to (-1)^l \, Q_{lm}$$
$$M_{lm} \to (-1)^{l+1} \, M_{lm}$$

The electric charge density $\rho_e(\hat{\boldsymbol{r}})$ is **time-reversal-even** and **parity-even,** such that

$\rho_e(\hat{\boldsymbol{r}}) = \rho_e(-\hat{\boldsymbol{r}})$ in the presence of inversion symmetry

And

$$\rho_e(\hat{\boldsymbol{r}}) = \sum_{l=0}^{\infty} \sum_{l=-m}^{m} (2l+1) \frac{Q_{lm}}{e\langle r^l \rangle} Z_{lm}(\hat{\boldsymbol{r}})$$

Electric multipoles are **time-reversal even**, and only **even-rank** electric multipoles are non-zero with inversion symmetry.

The magnetization density $\rho_m(\hat{\boldsymbol{r}})$ is **time-reversal-odd** and **parity-odd,** such that

$\rho_m(\hat{\boldsymbol{r}}) = -\rho_m(-\hat{\boldsymbol{r}})$ in the presence of inversion symmetry

And

$$\rho_m(\hat{\boldsymbol{r}}) = \sum_{l=0}^{\infty} \sum_{l=-m}^{m} (2l+1) \frac{M_{lm}}{\mu_B \langle r^{l-1} \rangle} Z_{lm}(\hat{\boldsymbol{r}})$$

Magnetic multipoles are time reversal odd, and only **odd-rank** magnetic multipoles are non-zero with inversion symmetry.

Symmetry properties of atomic multipoles?

Under inversion (spatial parity) transformation:

$$Q_{lm} \rightarrow (-1)^{l}\, Q_{lm}$$
$$M_{lm} \rightarrow (-1)^{l+1}\, M_{lm}$$

With an inversion-symmetric crystalline electric field (CEF), the local electron wavefunction has definite parity

→ **Even-rank** and **odd-rank** multipoles are **electric** and **magnetic** multipolar moments, respectively.

Only **even-rank** electric multipoles are non-zero

Only **odd-rank** magnetic multipoles are non-zero

Symmetry properties of atomic multipoles?

$\rho_e(\hat{\boldsymbol{r}}),\ \phi(\hat{\boldsymbol{r}}) =$

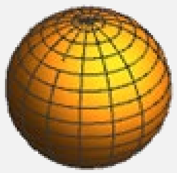

$l = 0$ (monopole)

$+$

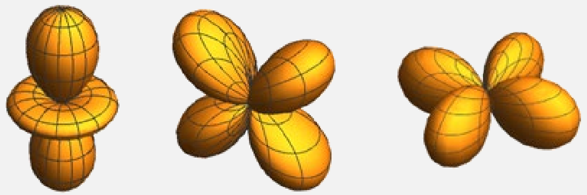

$l = 2$ (quadrupole)

Electrical d.o.f

$+$

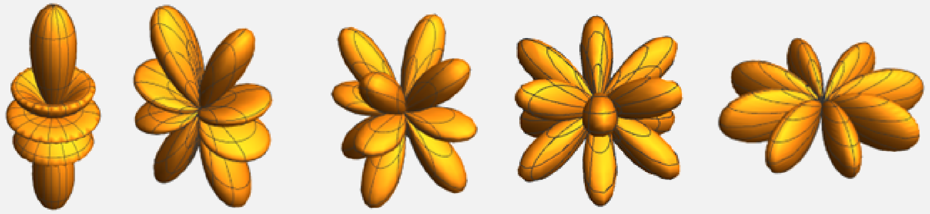

$l = 4$ (Hexadecapole) $+ \cdots$

$\rho_m(\hat{\boldsymbol{r}}),\ \boldsymbol{A}(\hat{\boldsymbol{r}}) =$

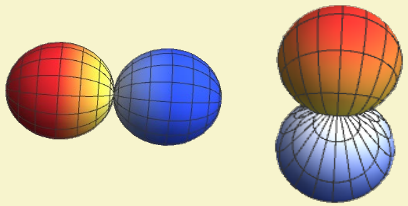

$l = 1$ (dipole/spin)

$+$

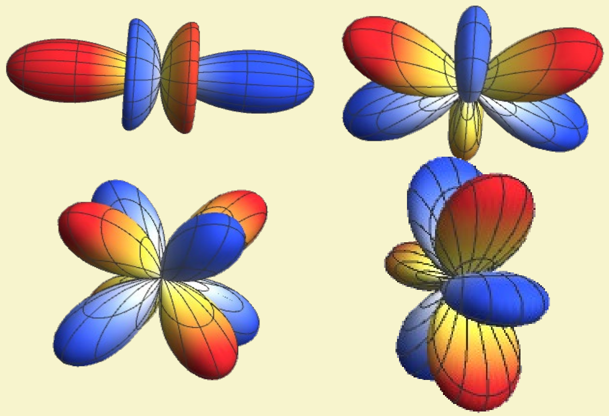

$l = 3$ (octupole) $+ \cdots$

Magnetic d.o.f

Platforms to explore atomic multipoles?

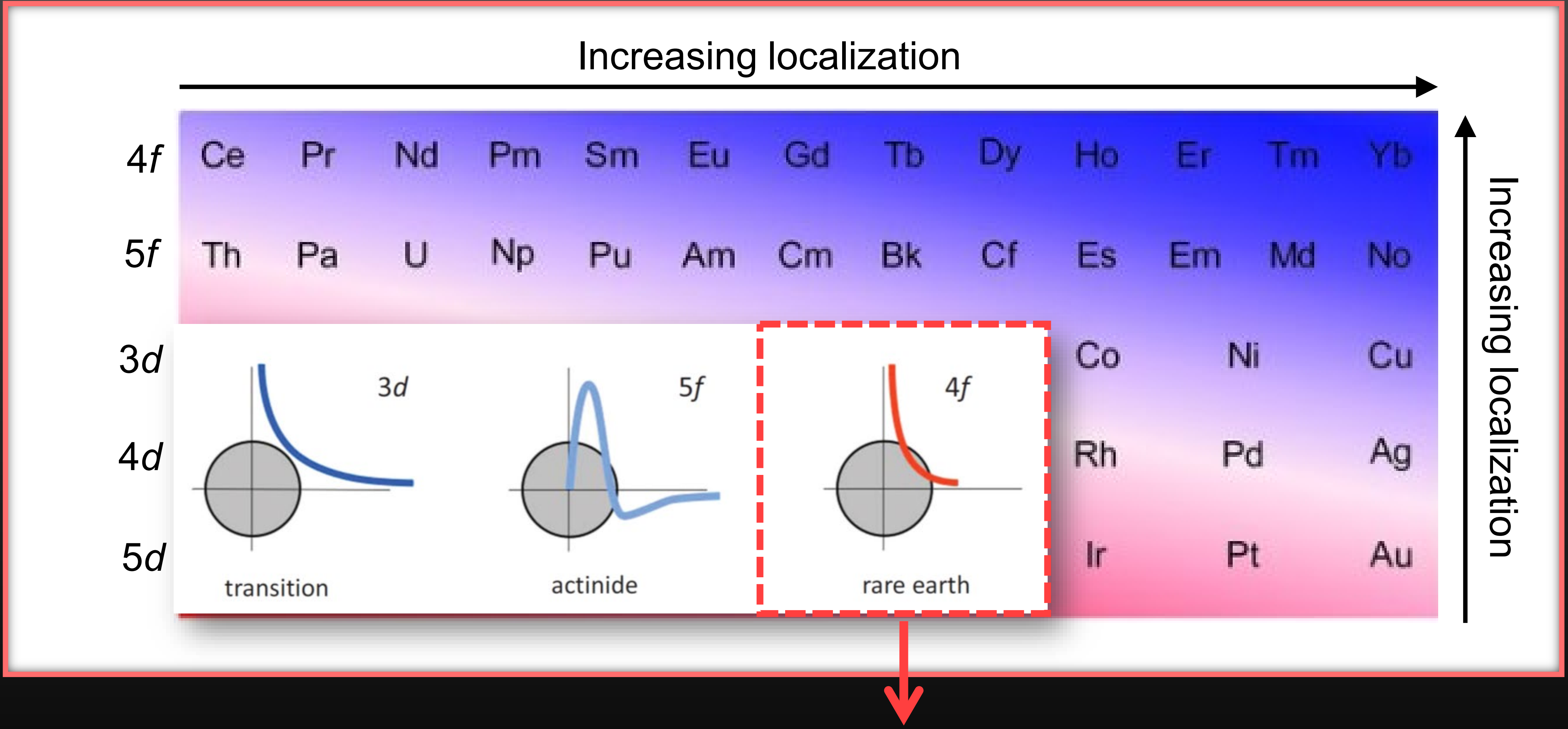

Large electron-electron interaction (Coulomb repulsion U ~ 1eV)

Large spin-orbit coupling ($\lambda_{SO} \sim Z^4$)

Highly localized electronic wavefunction at the atomic sites

Effects of crystalline electric field (CEF)

Crystalline Electric Field (CEF):

Modifies the energy levels of the electronic orbitals according to the **local symmetry** of the ion's environment in a crystal.

$$\mathcal{H}_{\mathrm{CEF}} = \sum_i q_i \phi(\boldsymbol{R}_i)$$

Stevens' operator O_{lm} →

$$\mathcal{H}_{\mathrm{CEF}} = \sum_{l,m} B_{lm} O_{lm}$$

Scalar potential at the ligand position $\boldsymbol{R}_i$ created by the magnetic ion

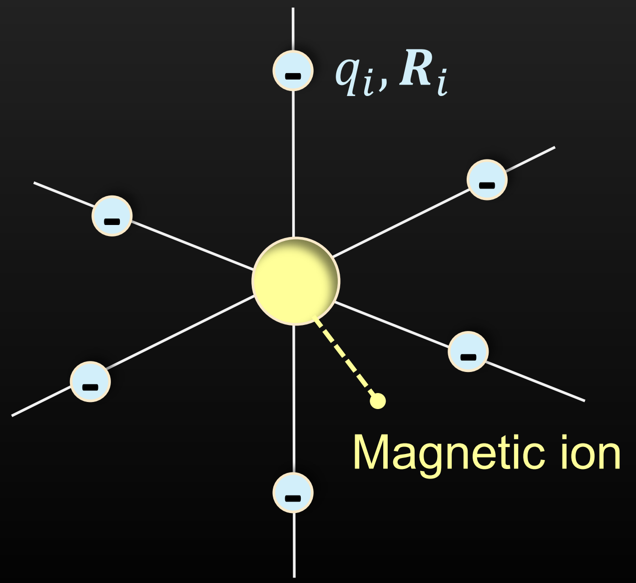

Example: Local cubic symmetry (T_d and O_h)

$$\mathcal{H}_{\mathrm{CEF}} = B_{40}(O_{40} + 5O_{44}) + B_{60}(O_{60} - 21O_{64})$$

Effects of crystalline electric field (CEF)

Crystalline Electric Field (CEF):

Modifies the energy levels of the electronic orbitals according to the **local symmetry** of the ion's environment in a crystal.

Example: *d*-orbital splitting due to CEF

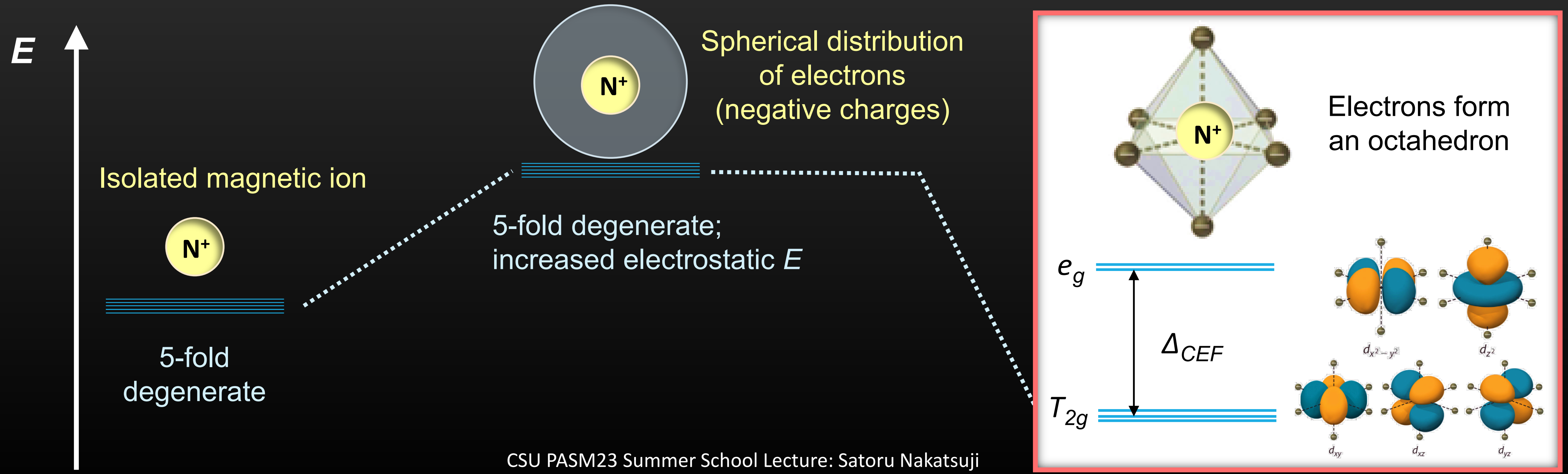

Example: Ce^{3+} in a cubic CEF

Ce^{3+} ($4f^1$): $L = 3$, $S = 1/2$, $J = 5/2$

The CEF Hamiltonian in the basis set for $J = 5/2$:

$$\mathcal{H}_{\mathrm{CEF}} = B_{40}\begin{pmatrix} 60 & 0 & 0 & 0 & 60\sqrt{5} & 0 \\ 0 & -180 & 0 & 0 & 0 & 60\sqrt{5} \\ 0 & 0 & 120 & 0 & 0 & 0 \\ 0 & 0 & 0 & 120 & 0 & 0 \\ 60\sqrt{5} & 0 & 0 & 0 & -180 & 0 \\ 0 & 60\sqrt{5} & 0 & 0 & 0 & 60 \end{pmatrix}$$

Solve the eigenvalue problem

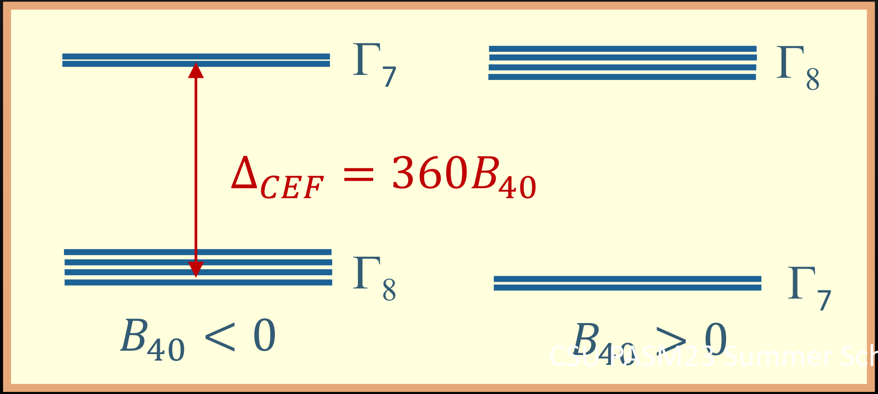

$$|\Gamma_7^{\pm}\rangle = \frac{1}{\sqrt{6}}\left|\pm\frac{5}{2}\right\rangle - \sqrt{\frac{5}{6}}\left|\mp\frac{3}{2}\right\rangle$$

$$|\Gamma_8^{\pm}, a\rangle = \sqrt{\frac{5}{6}}\left|\pm\frac{5}{2}\right\rangle + \frac{1}{\sqrt{6}}\left|\mp\frac{3}{2}\right\rangle \qquad |\Gamma_8^{\pm}, b\rangle = \left|\pm\frac{1}{2}\right\rangle$$

Example: Ce^{3+} in a cubic CEF

Charge and magnetization density distribution for $|\Gamma_7^{\pm}\rangle, |\Gamma_8^{\pm}, a\rangle, |\Gamma_8^{\pm}, b\rangle$

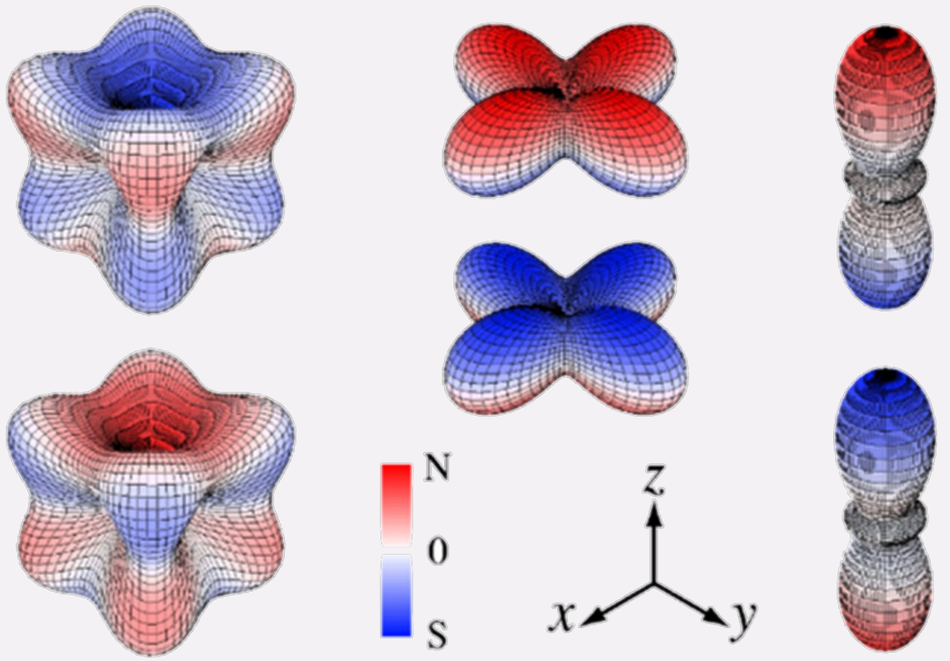

Representative multipoles of Γ_8 quartet

O_h multipole[a] (degeneracy)	rank p	Stevens notation J_α, $(\alpha = x, y, z)$
$\Gamma_4^-(3)$	1 (d)	J_x J_y J_z
$\Gamma_3^+(2)$	2 (q)	$O_2^0 = \frac{1}{2}(2J_z^2 - J_x^2 - J_y^2)$ $O_2^2 = \frac{\sqrt{3}}{2}(J_x^2 - J_y^2)$
$\Gamma_5^+(3)$	2 (q)	$O_{yz} = \frac{\sqrt{3}}{2}(J_yJ_z + J_zJ_y)$ $O_{zx} = \frac{\sqrt{3}}{2}(J_zJ_x + J_xJ_z)$ $O_{xy} = \frac{\sqrt{3}}{2}(J_xJ_y + J_yJ_x)$
$\Gamma_2^-(1)$	3 (o)	$T_{xyz} = \frac{\sqrt{15}}{6}\overline{J_xJ_yJ_z}$

Dipole

Quadrupole

Octupole

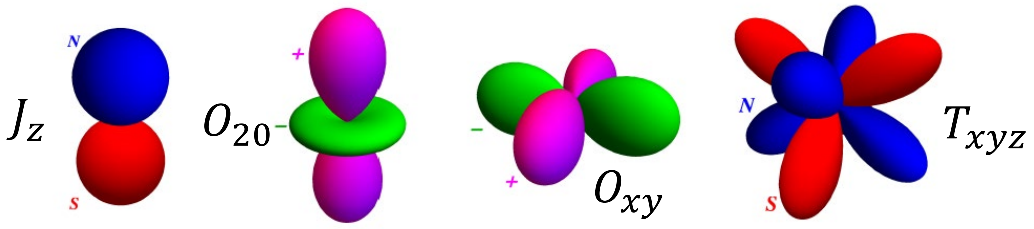

H. Kusunose, J. Phys. Soc. Jpn. **77**, 064710 (2008)

P. Thalmeier *et al.*, arXiv:1907.10967

Multipolar phenomena in Ce^{3+}-based systems

La-doped CeB_6 : *B*-*T* phase diagram featuring dipolar, quadrupolar, and octupolar orders

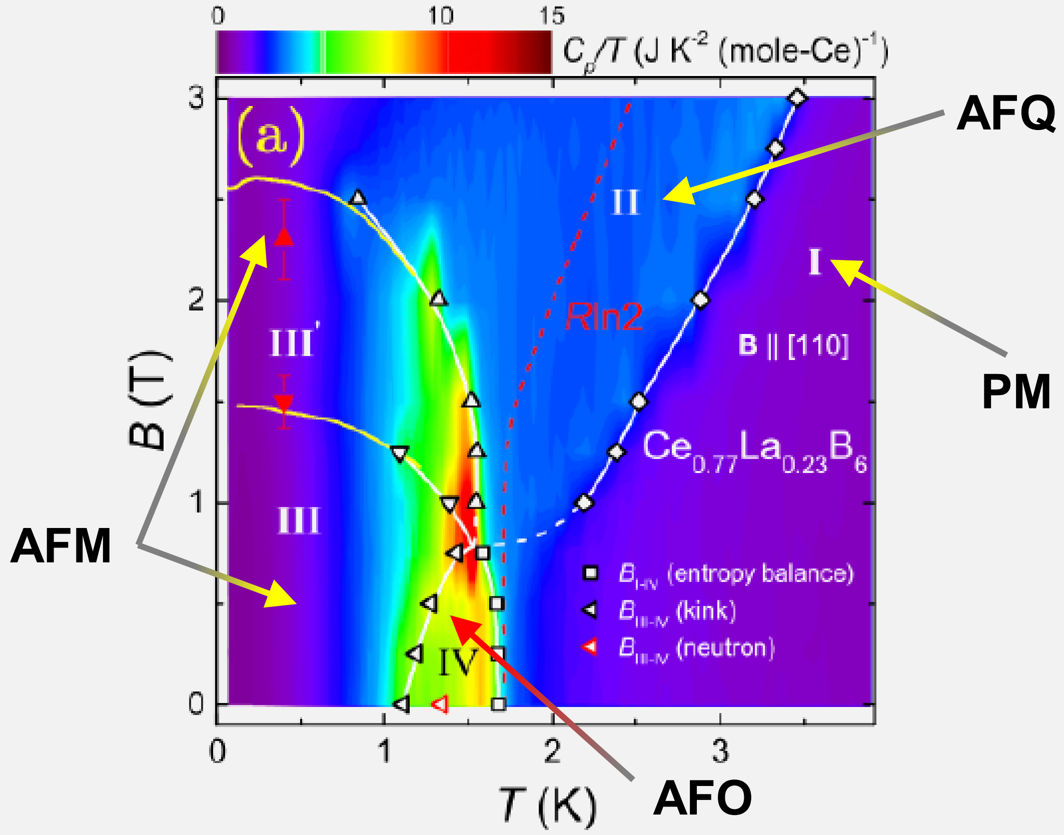

$Ce_3Pd_{20}Si_6$: Two electron localization transitions driven by dipolar and quadrupolar d.o.f

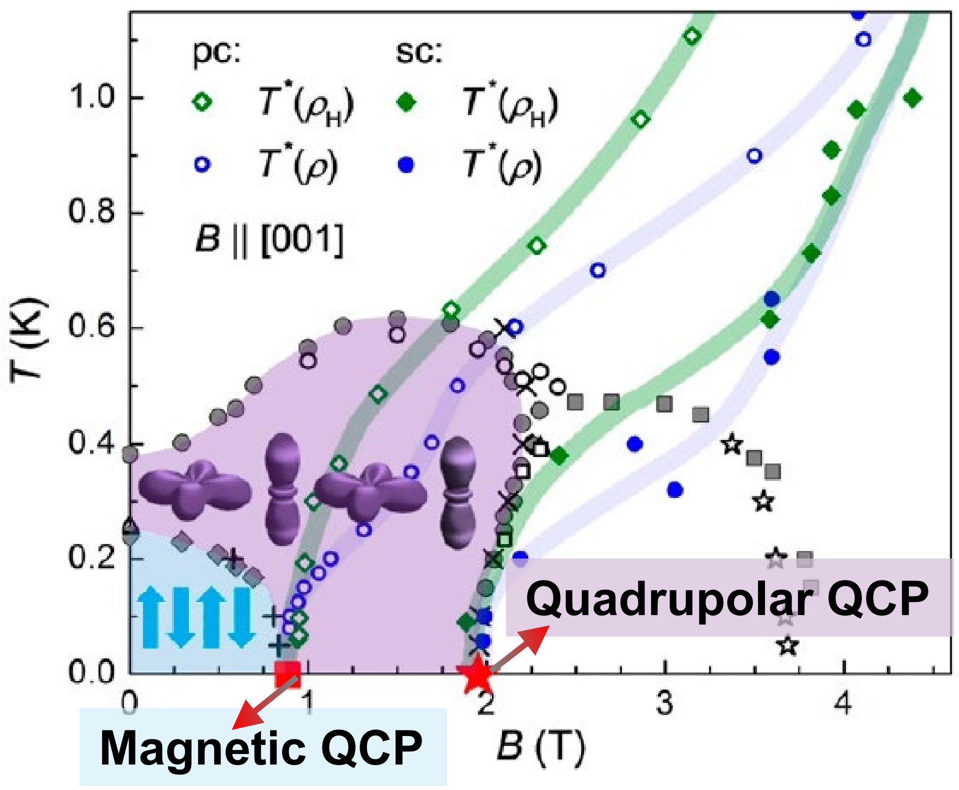

D. Jang et al., npj Quantum Mater (2017)

V. Martellia et al., PNAS (2019)

Multipolar phenomena in Ce^{3+}-based systems

La-doped CeB_6 : *B*-*T* phase diagram featuring dipolar, quadrupolar, and octupolar orders

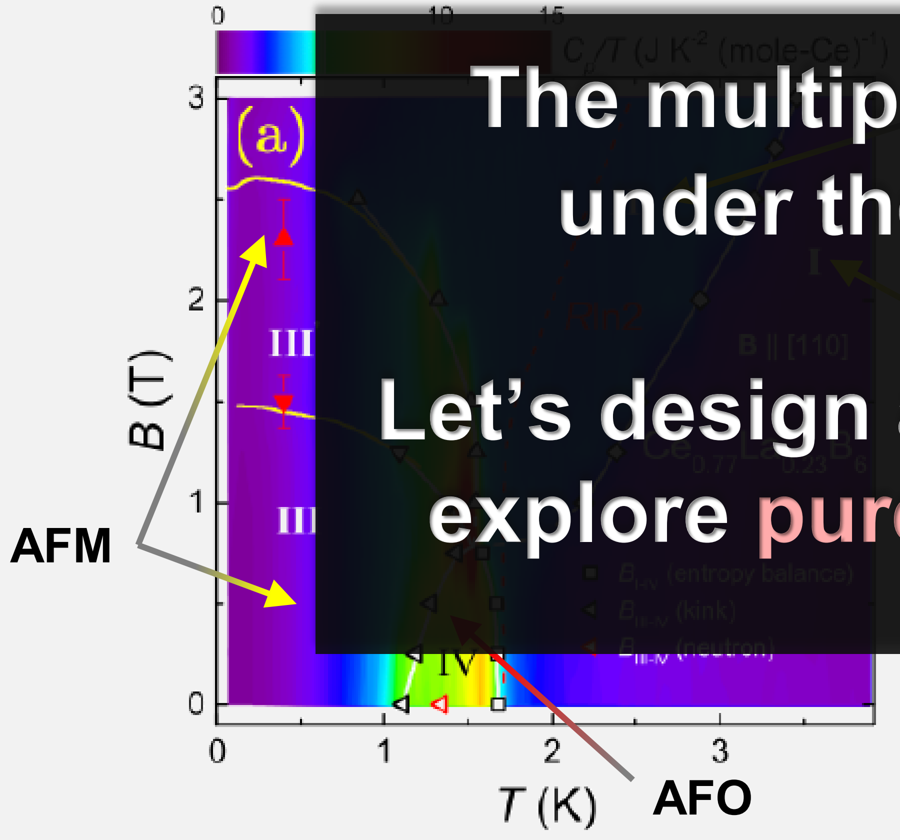

D. Jang et al., npj Quantum Mater (2017)

$Ce_3Pd_{20}Si_6$: Two electron localization transitions driven by dipolar and quadrupolar d.o.f

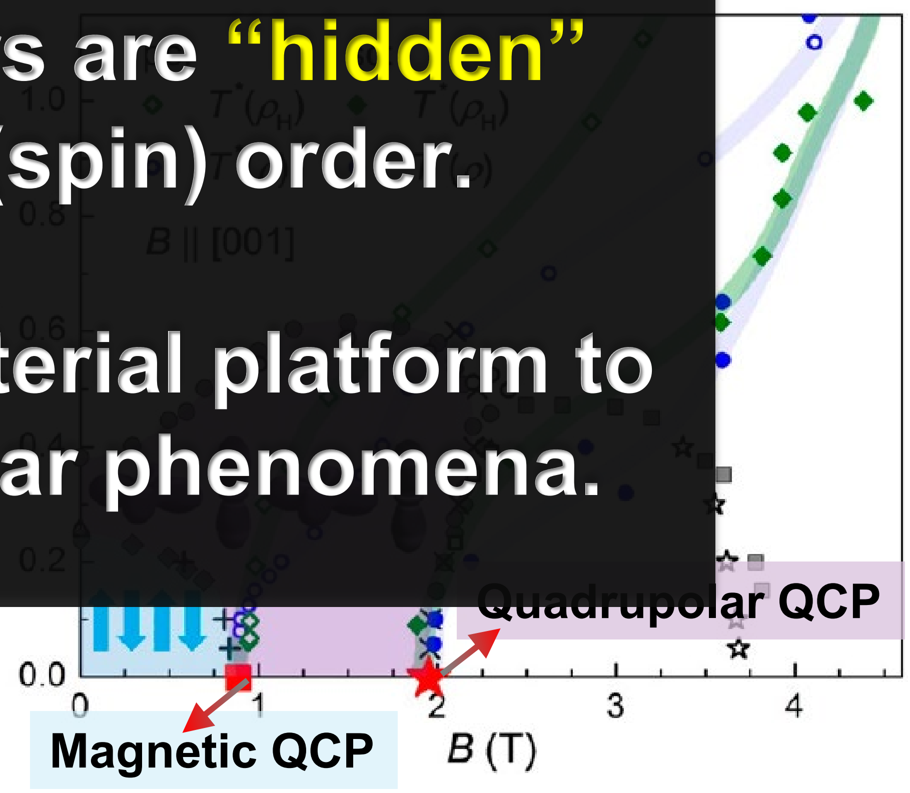

V. Martellia et al., PNAS (2019)

The multipolar orders are "hidden" under the dipolar (spin) order.

Let's design a new material platform to explore pure multipolar phenomena.

Cubic Pr^{3+} systems: Ideal platform for multipolar physics

4*f* Kramers doublet (e.g., Ce^{3+}, Yb^{3+})

- Odd number of f electrons
- Half-integer *J*
- Kramer's theory: **double degeneracy protected by time-reversal symmetry**

Ce^{3+} ($4f^1$) *J* = 7/2

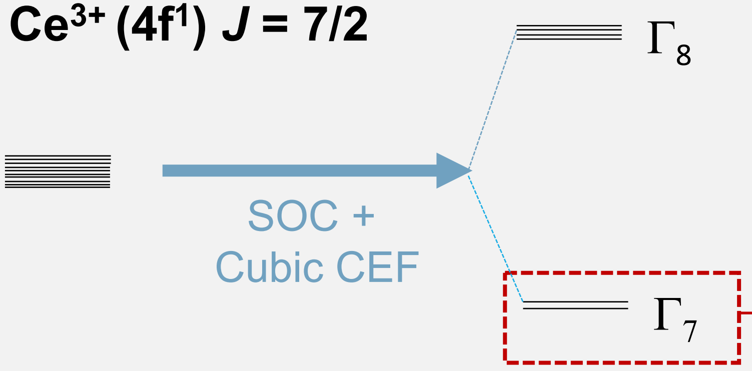

Always carry magnetic dipoles

Degeneracy is robust against structural disorder

4*f* non-Kramers doublet (e.g., Pr^{3+})

- Even number of f electrons
- Integer *J*
- Double degeneracy is ***not*** protected by time-reversal symmetry but by **the local symmetry**

Pr^{3+} ($4f^2$) *J* = 5

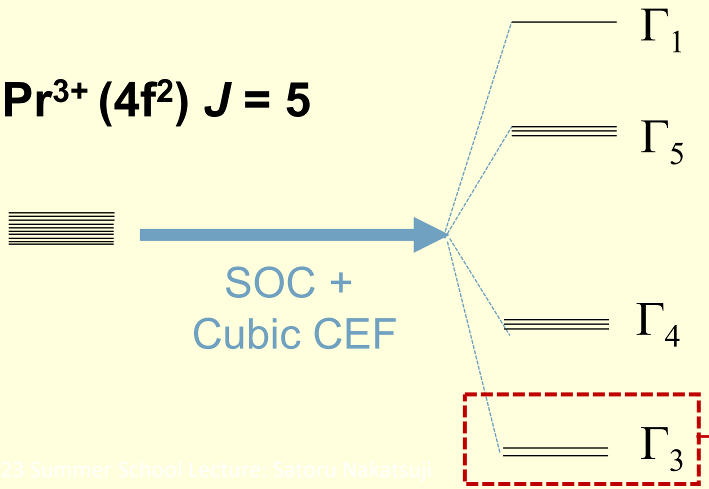

No magnetic dipoles but high-rank multipoles

Degeneracy can be lifted by structural disorder

Cubic Pr^{3+} systems: Ideal platform for multipolar physics

Pr $(TM)_2Al_{20}$

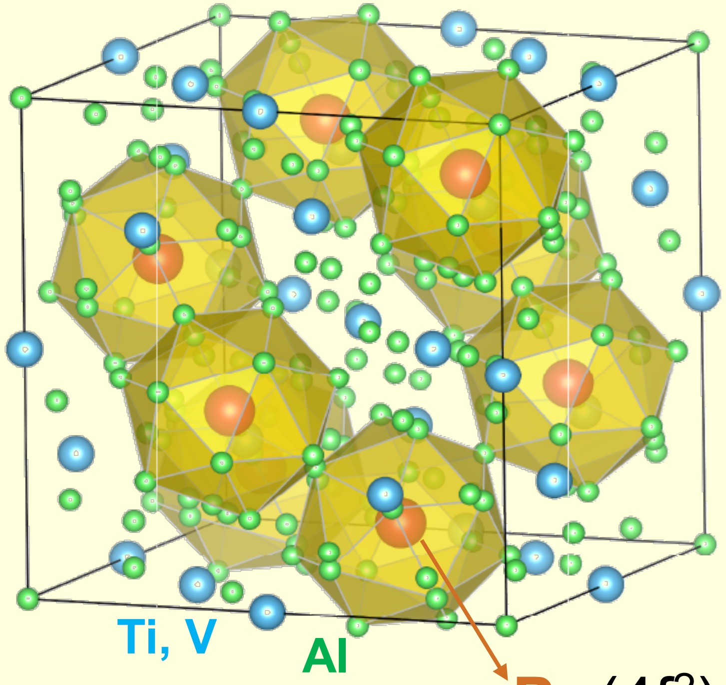

Frank-Kasper cages of 16 Al surrounding the Pr ion → strong *c-f* hybridization

CEF scheme of Pr^{3+} in local **cubic** environment

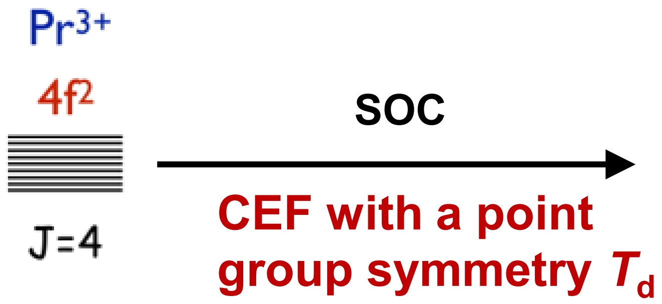

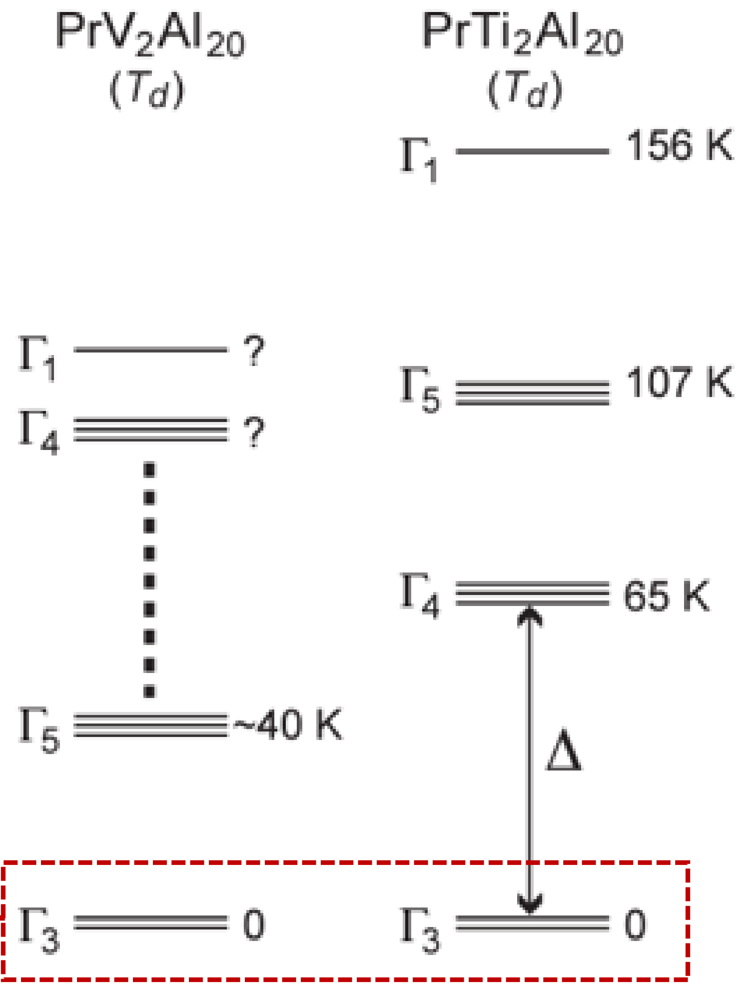

$$|\Gamma_3^+\rangle = \frac{1}{2}\sqrt{\frac{7}{6}}(|+4\rangle + |-4\rangle) - \frac{1}{2}\sqrt{\frac{5}{3}}|0\rangle$$

$$|\Gamma_3^-\rangle = \sqrt{\frac{1}{2}}(|+2\rangle + |-2\rangle)$$

Well-isolated non-Kramers doublet ground state

Active multipoles in cubic Pr^{3+} systems

Basis states of the Γ_3 non-Kramers doublet: $|\Gamma_3\rangle = \begin{pmatrix} |\Gamma_3^+\rangle \\ |\Gamma_3^-\rangle \end{pmatrix}$

$\langle\Gamma_3^\pm | J_\alpha |\Gamma_3^\pm\rangle = 0$, where $\alpha = x, y, z$ **No dipole moment!**

Finite matrix elements for

Quadrupolar moments (time-reversal even)

$$O_{22} \equiv \frac{\sqrt{3}}{2}(J_x^2 - J_y^2) \qquad O_{20} \equiv \frac{1}{2}(3J_z^2 - J^2)$$

Octupolar moment (time-reversal odd)

$$T_{xyz} \equiv \frac{\sqrt{15}}{6}\overline{J_x J_y J_z}$$

Pseudospin-1/2 basis

$$|\uparrow\rangle = \frac{1}{\sqrt{2}}(|\Gamma_3^+\rangle + i|\Gamma_3^-\rangle)$$

$$|\downarrow\rangle = \frac{1}{\sqrt{2}}(i|\Gamma_3^+\rangle + |\Gamma_3^-\rangle)$$

$$S^x = -\frac{1}{4}O_{22} \qquad S^y = -\frac{1}{4}O_{20} \qquad S^z = \frac{1}{3\sqrt{5}}T_{xyz}$$

Cubic Pr^{3+} systems: Ideal platform for multipolar physics

$Pr(TM)_2Al_{20}$

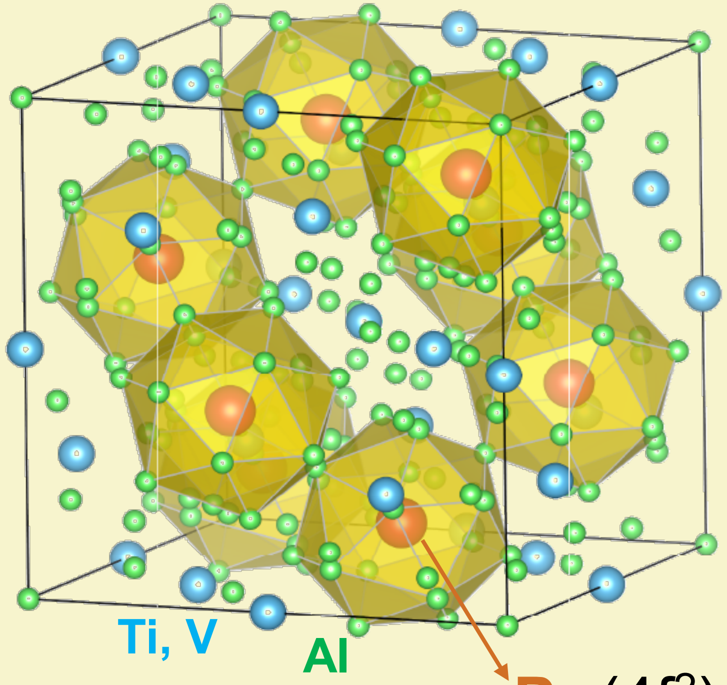

Frank-Kasper cages of 16 Al surrounding the Pr ion
→ strong *c-f* hybridization

CEF scheme of Pr^{3+}
in local **cubic**
environment

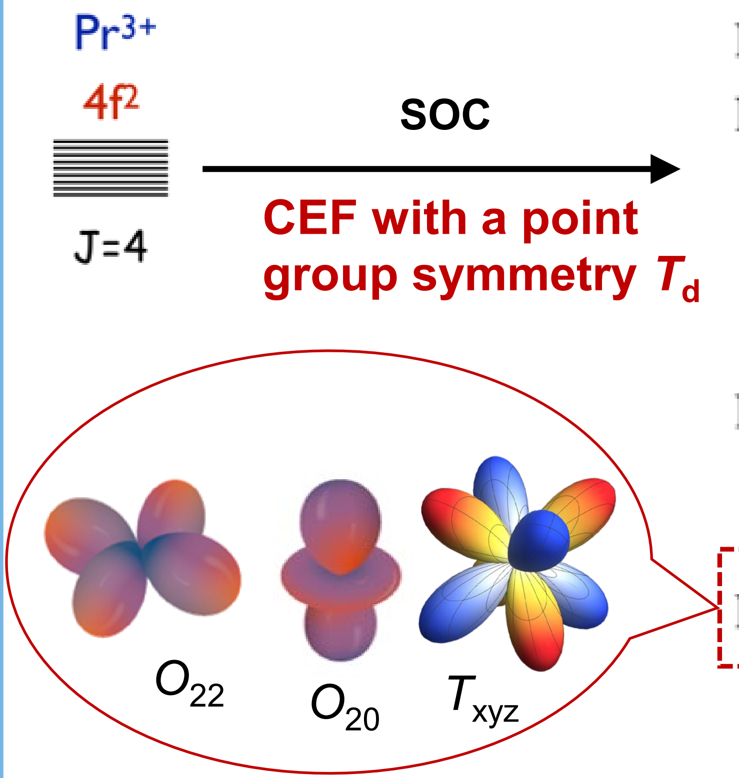

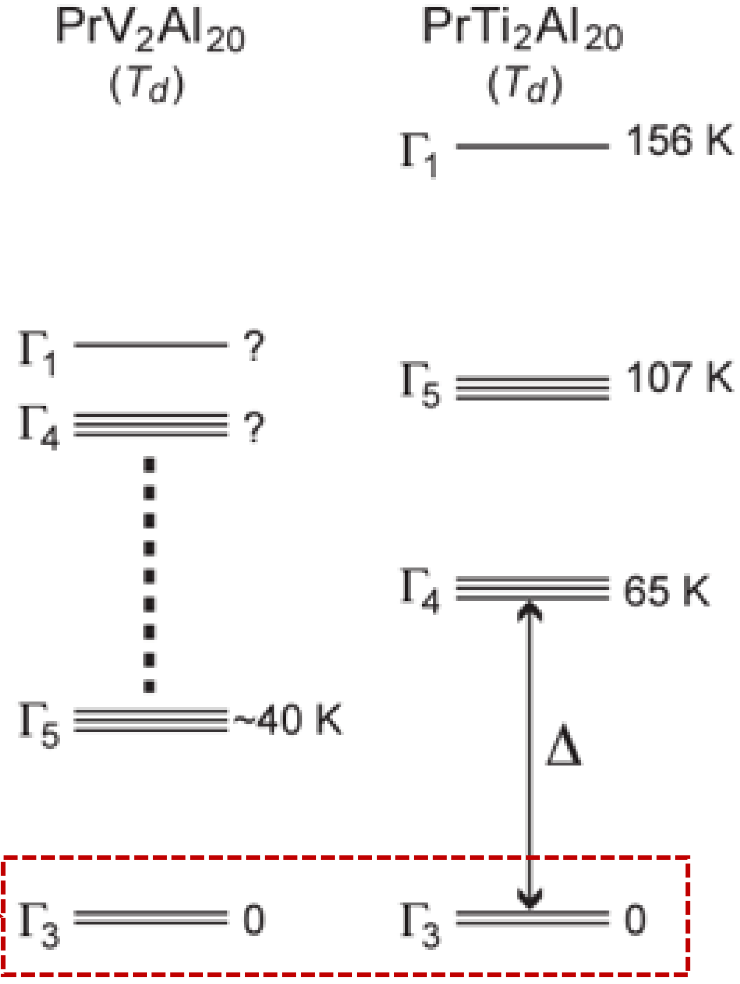

Non-magnetic!

Probing atomic multipoles

- Long-range ordered phases involving high-rank multipoles are often referred to as **"hidden orders"** because their nature is **highly challenging to detect using conventional magnetic probes**, such as neutron scattering

- **Lattice strains w** **with the order pa** magnetic field on

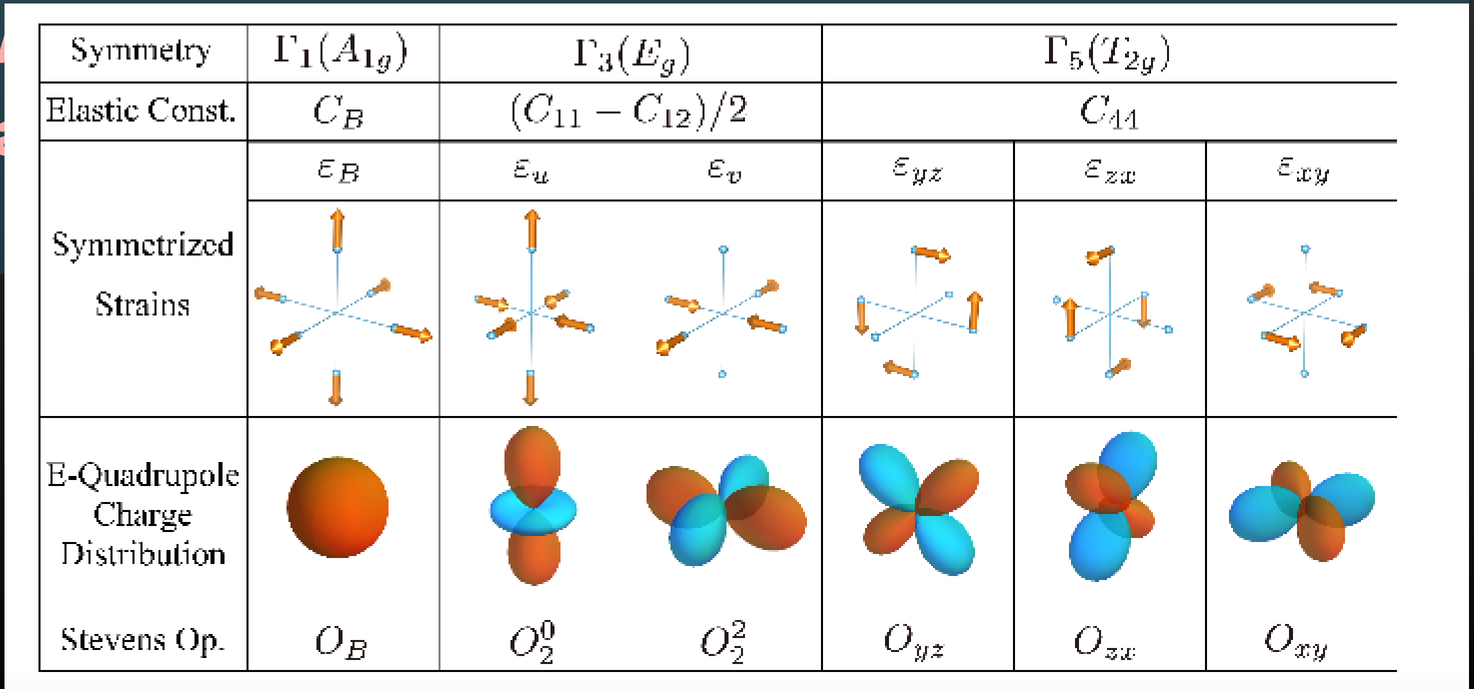

Symmetry	$\Gamma_1(A_{1g})$	$\Gamma_3(E_g)$		$\Gamma_5(T_{2g})$		
Elastic Const.	C_B	$(C_{11}-C_{12})/2$		C_{44}		
Symmetrized Strains	ε_B	ε_u	ε_v	ε_{yz}	ε_{zx}	ε_{xy}
E-Quadrupole Charge Distribution						
Stevens Op.	O_B	O_2^0	O_2^2	O_{yz}	O_{zx}	O_{xy}

T. Yanagisawa *et al.*, PRL**123**, 067201, (2019)

Probing atomic multipoles

- Long-range ordered phases involving high-rank multipoles are often referred to as **"hidden orders"** because their nature is **highly challenging to detect using conventional magnetic probes**, such as neutron scattering

- **Lattice strains with appropriate symmetries can directly couple with the order parameter of multipolar order**, like the effect of a magnetic field on dipolar moments.

Measurement of elastic modulus (e.g., ultrasound, magnetostriction) ↔ **Ordering of high-rank atomic multipoles**

Probing multipole order with ultrasound

What can we learn from the ultrasound?

→ Elastic constant $C = v^2 \rho$

Sound velocity (v^2) Density (ρ)

	Electric Quadrupole	Magnetic dipole
Field	Lattice strain ϵ_Γ	Magnetic field *H*
Order parameter	$\langle O_\Gamma \rangle = \frac{\partial F}{\partial \epsilon_\Gamma}$	$\langle M \rangle = -\frac{\partial F}{\partial H}$
	$\chi_\Gamma = -\frac{1}{g_\Gamma^2}\frac{\partial^2 F}{\partial \epsilon_\Gamma^2} = -\frac{1}{g_\Gamma^2} C_\Gamma$	$\chi = -\frac{\partial^2 F}{\partial H^2}$

Elastic constant directly probes the quadrupolar susceptibility!

Probing multipole order with ultrasound

What can we learn from the ultrasound?

→ Elastic constant $C = v^2\rho$

Sound velocity (v^2) Density (ρ)

	Electric Quadrupole	Magnetic dipole
Field	Lattice strain ϵ_Γ	Magnetic field ***H***
Order parameter	$\langle O_\Gamma \rangle = \frac{\partial F}{\partial \epsilon_\Gamma}$	$\langle M \rangle = -\frac{\partial F}{\partial H}$
	$\chi_\Gamma = -\frac{1}{g_\Gamma^2}\frac{\partial^2 F}{\partial \epsilon_\Gamma^2} = -\frac{1}{g_\Gamma^2} C_\Gamma$	$\chi = -\frac{\partial^2 F}{\partial H^2}$

Elastic constant directly probes the quadrupolar susceptibility!

Example: spin-orbital liquid in Pr^{3+}-based pyrochlore

Spin–orbital interlocking in the non-Kramers doublet

N. Tang *et al.*, Nat. Phys (2022)

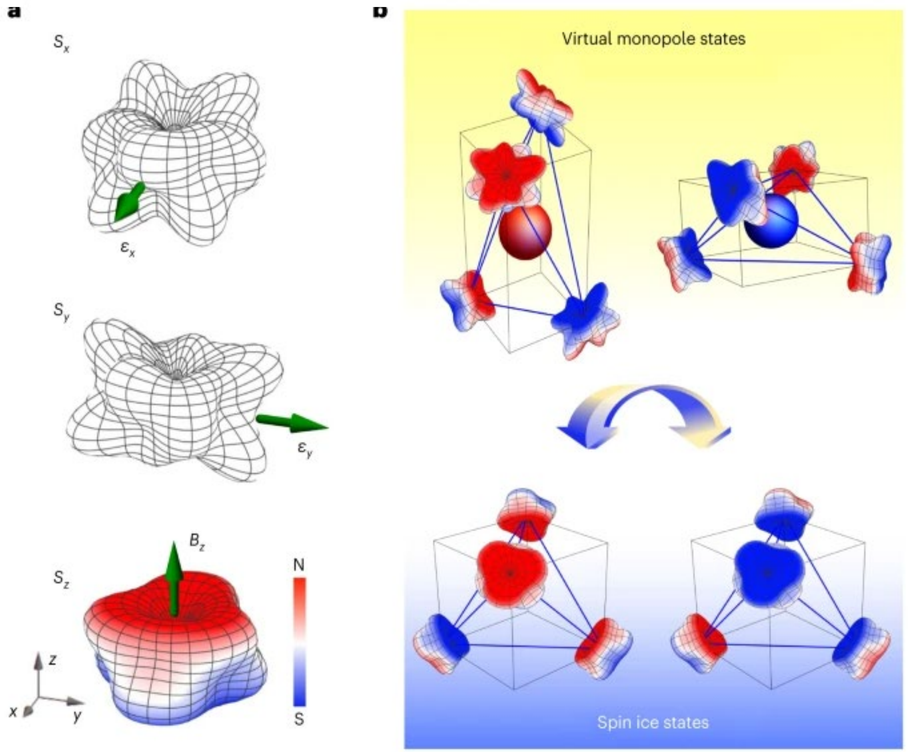

The non-Kramers doublet in $Pr_2Zr_2O_7$ hosts two **time-reversal even quadrupolar moments** (XY pseudospin components) and (Z pseudospin component) **one time-reversal odd dipolar moment**

Strong lattice softening accompanying the liquid-gas metamagnetic transition

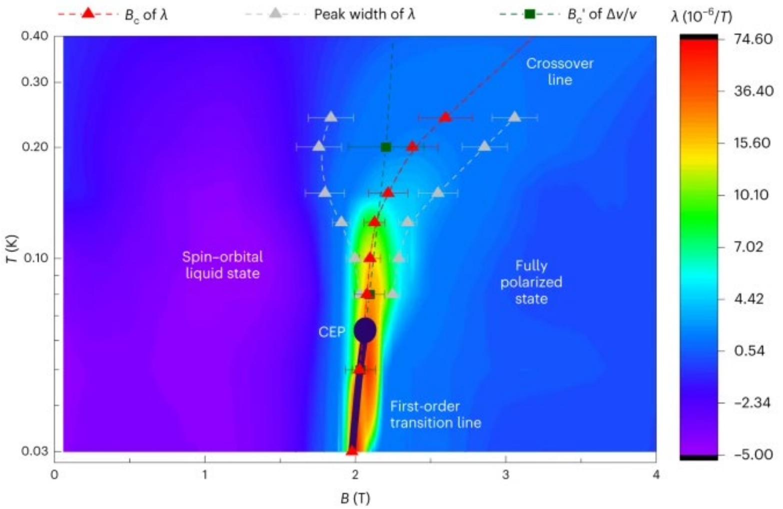

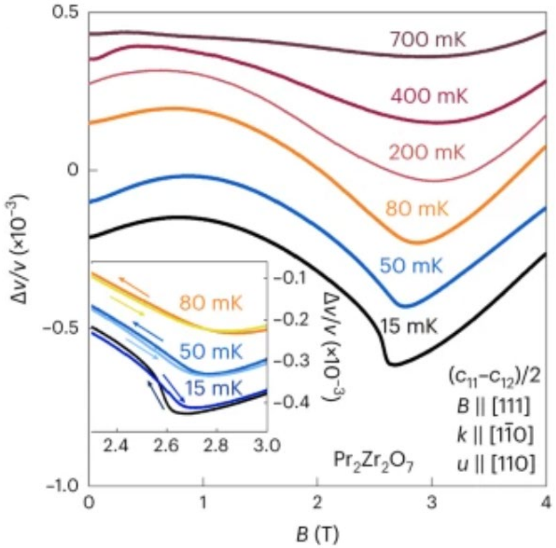

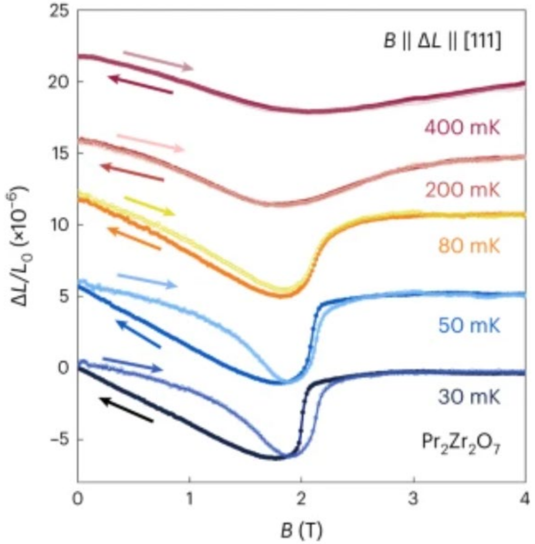

Example: spin-orbital liquid in Pr^{3+}-based pyrochlore

Spin–orbital interlocking in the non-Kramers doublet

N. Tang *et al.,* Nat. Phys (2022)

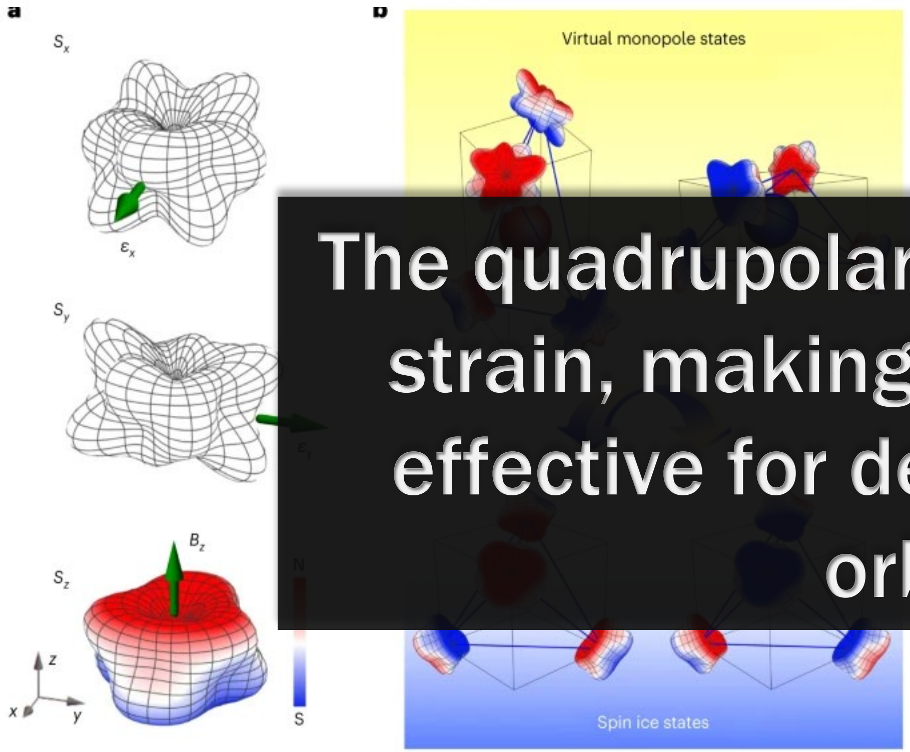

The non-Kramers doublet in $Pr_2Zr_2O_7$ hosts two **time-reversal even quadrupolar moments** (XY pseudospin components) and (Z pseudospin component) **one time-reversal odd dipolar moment**

Strong lattice softening accompanying the liquid-gas metamagnetic transition

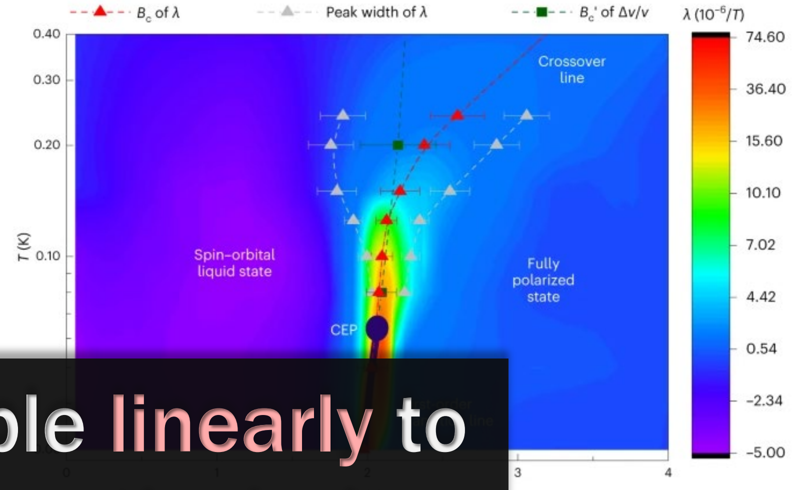

The quadrupolar moments couple **linearly** to strain, making **lattice probes** particularly effective for detecting the low-lying spin-orbital dynamics

Ultrasound velocity

Magnetostriction

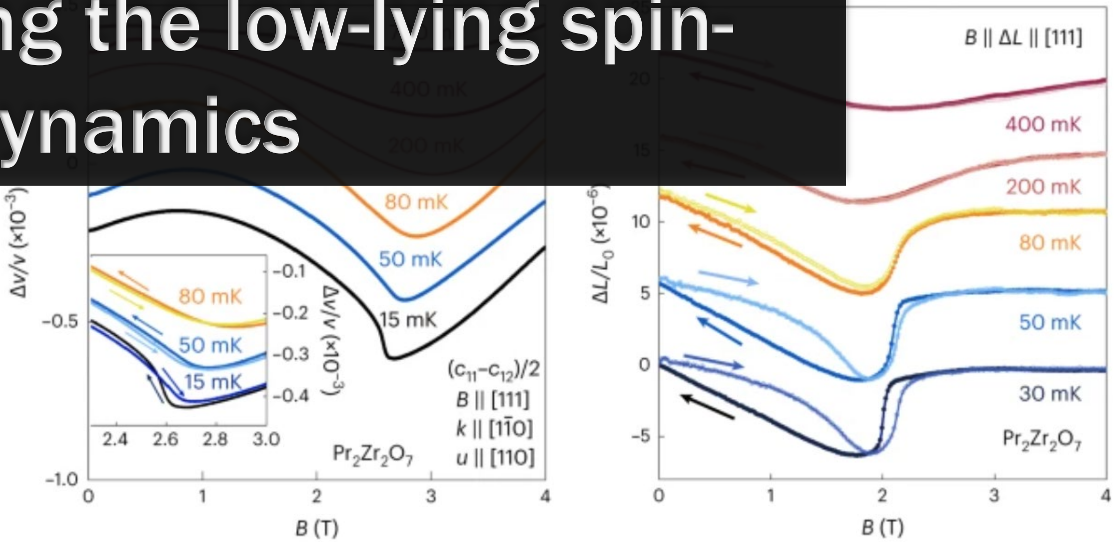

How do multipoles modify quantum phenomena?

Magnetic Kondo effect

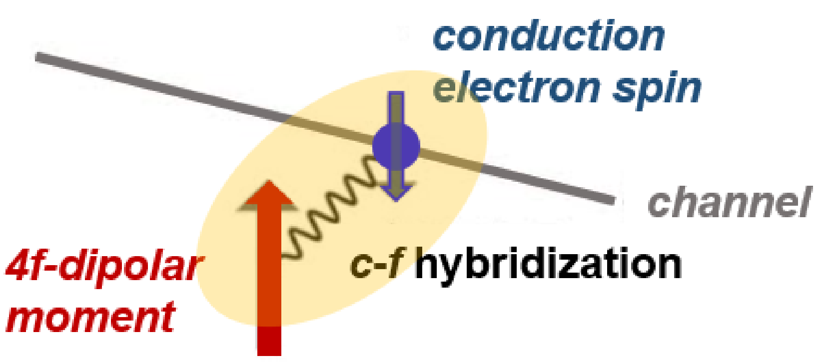

Single-channel Kondo model (k = 1) and **exact screening**

f electrons become itinerant and enter the Fermi surface in the **heavy-fermion Fermi liquid (FL) ground state**

$$\rho \sim AT^2 \qquad C/T \sim \frac{m^*}{m_0}\gamma_0$$

VS.

Quadrupolar Kondo effect

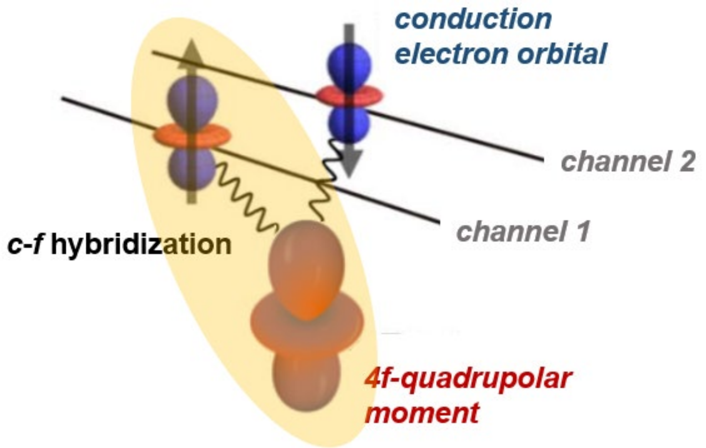

Two-channel Kondo model (k = 2) and **over-screening** D. L. Cox, Phys. Rev. Lett. (1987).

Residual entropy $S_0 = \frac{1}{2}R\ln 2$ **leads to a non-Fermi liquid (NFL) ground state**

$$\rho \sim T^{1/2},\ C/T \sim -\ln T,$$
$$\chi \sim T^{1/2} \text{ or } \sim -\ln T$$

How do multipoles modify quantum phenomena?

Magnetic Kondo effect

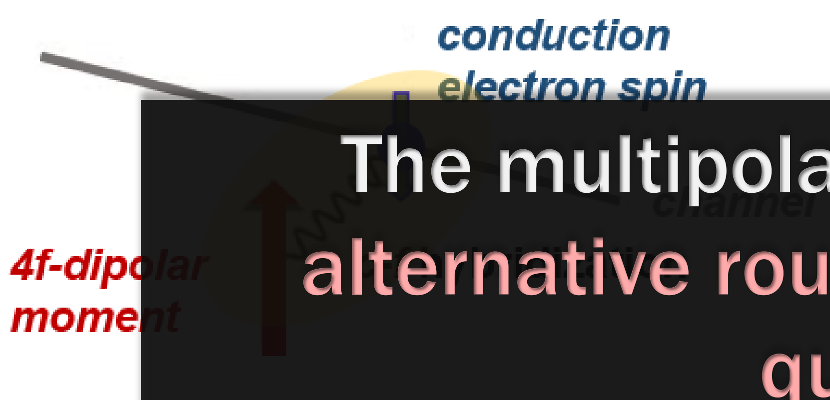

Single-channel ... **and exact screening**

f electrons ... the Fermi ... **Fermi liquid (FL) ground state**

$$\rho \sim AT^2 \qquad C/T \sim \frac{m^*}{m_0}\gamma_0$$

Quadrupolar Kondo effect

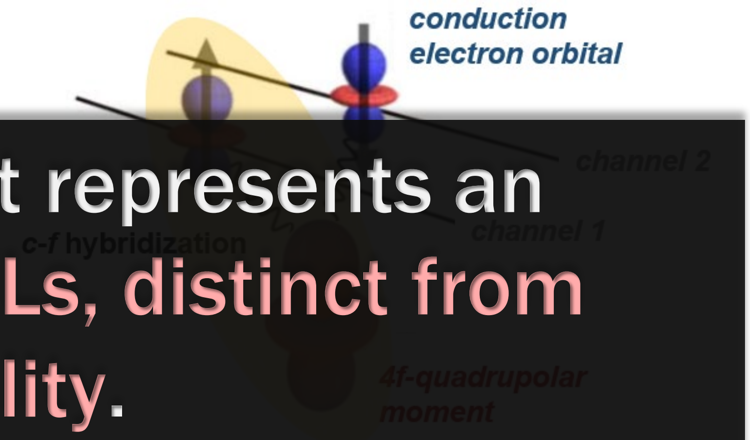

... (k = 2) and ... over-screening ... 1987).

... to a ... non-Fermi liquid (NFL) ground state

$$\rho \sim T^{1/2},\ C/T \sim -\ln T,$$

$\chi \sim T^{1/2}$ or $\sim -\ln T$

The multipolar Kondo effect represents an alternative route to novel NFLs, distinct from quantum criticality.

The NFL is intrinsic to the multipolar Kondo interaction and thus does not require fine-tuning of parameters.

Multipolar RKKY vs. Multipolar Kondo effect?

Modulated AFQ order in $PrPb_3$

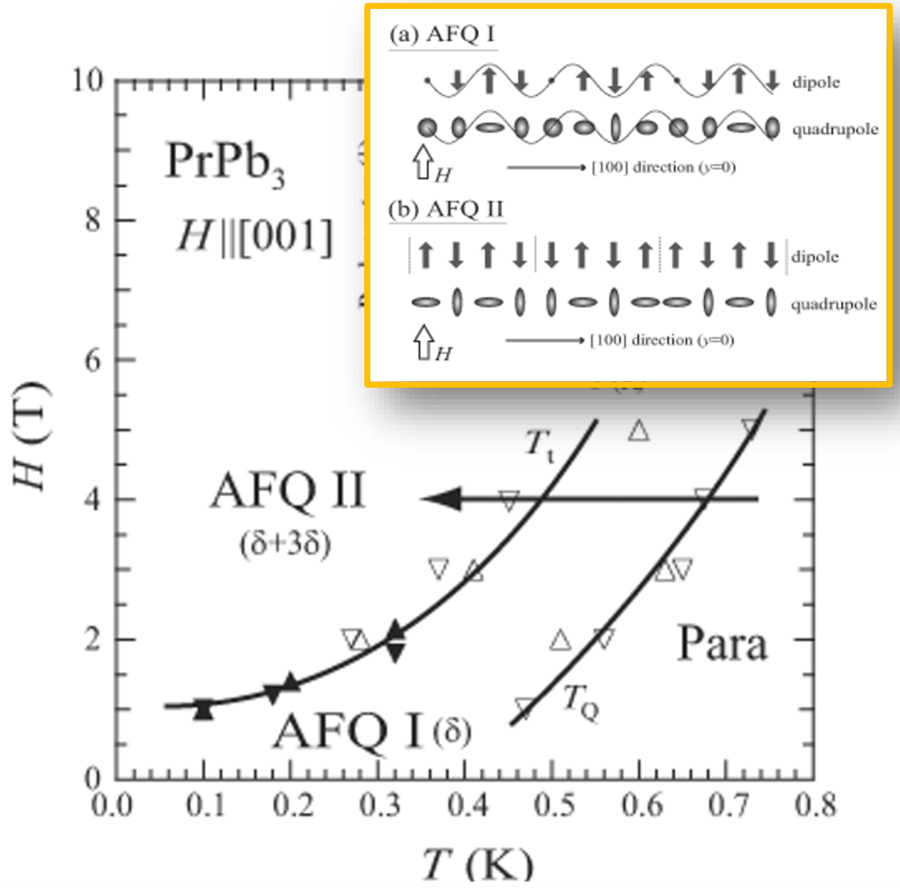

T. Ominaru *et al.*, PRL**94**, 197201 (2005)

Single-site multipolar Kondo effect in $Y_{1-x}Pr_xIr_2Zn_{20}$

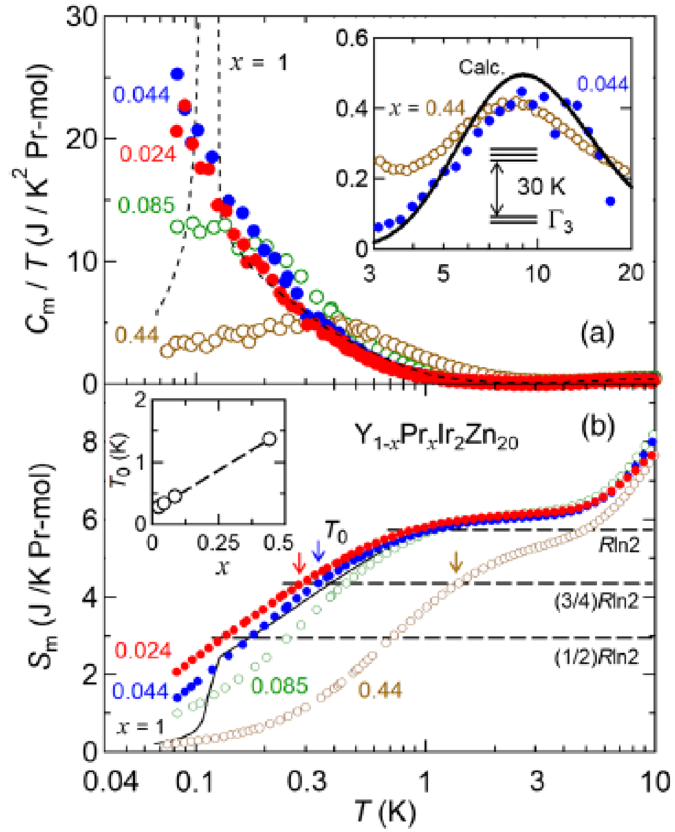

$PrIr_2Zn_{20}$ (x = 1)

AFQ order

Dilute

$Y_{1-x}Pr_xIr_2Zn_{20}$

Non-Fermi liquid

Y. Yamane *et al.*, PRL**121**, 077206 (2018)

Multipolar RKKY vs. Multipolar Kondo effect?

Modulated AFQ order in $PrPb_3$

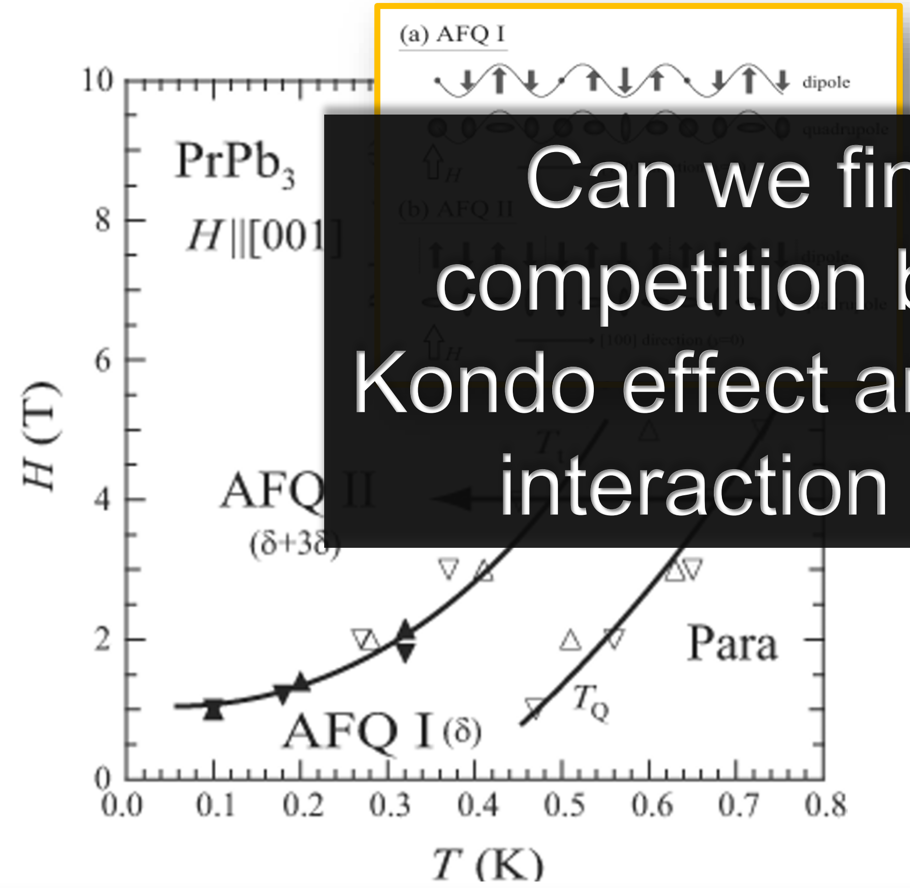

T. Ominaru *et al.*, PRL**94**, 197201 (2005)

Single-site multipolar Kondo effect in $Y_{1-x}Pr_xIr_2Zn_{20}$

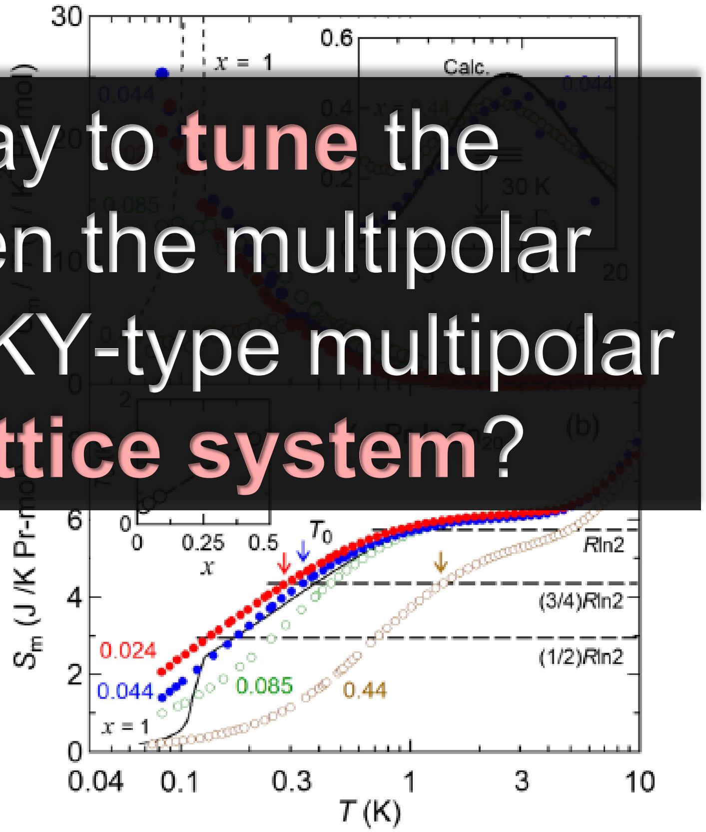

$PrIr_2Zn_{20}$ (x = 1)

AFQ order

Dilute

$Y_{1-x}Pr_xIr_2Zn_{20}$

Non-Fermi liquid

Can we find a way to **tune** the competition between the multipolar Kondo effect and RKKY-type multipolar interaction in **a lattice system**?

Y. Yamane *et al.*, PRL**121**, 077206 (2018)